Songklanakarin J. Sci. Technol.
43 (1), 222-228, Jan. - Feb. 2021

http://www.sjst.psu.ac.th

*Original Article*

# Modified montmorillonite with alkylamine chloroanthraquinone as a colorimetric sensor for detection and separation of $Cu^{2+}$ from an aqueous solution

Duangrat Thongkum[1*], Thitiporn Nomnuch[1], and Saksit Chuenchomnakjad[2]

[1] *Department of Chemistry, Faculty of Science, Naresuan University, Mueang, Phitsanulok, 65000 Thailand*

[2] *Program of Industrial Engineering, Rajamangala University of Technology Lanna, Phitsanulok Campus, Mueang, Phitsanulok, 65000 Thailand*

Received: 19 June 2019; Revised; 13 November 2019; Accepted: 7 December 2019

**Abstract**

To compare the adsorption capacity of $Cu^{2+}$ between Mt and Mt modified with alkylamine chloroanthraquinone for a colorimetric sensor (Mt-L), the adsorption by Mt and Mt-L of $Cu^{2+}$ was studied by using UV-vis spectroscopy. Their structures were characterized by FTIR spectroscopy and XRD techniques. Effects on the removal efficiency of $Cu^{2+}$ by adsorbent quantity, pH, initial $Cu^{2+}$ concentration, equilibrium adsorption time, adsorption kinetics, and adsorption isotherm were determined. The results revealed that the maximum adsorption efficiency was 54% with an initial $Cu^{2+}$ concentration of $3.50\times10^{-3}$ M, 40.0 g/L of Mt-L and an initial pH of 5.0. The adsorption kinetics were compatible with the pseudo-second order model and the adsorption isotherm with the Langmuir isotherm. The $q_m$ of Mt-L was calculated to be 9.5511 mg/g, which was higher than for the adsorption of $Cu^{2+}$ by Mt (2.6260 mg/g). Therefore, Mt-L has great potential as an adsorbent of $Cu^{2+}$ ions in aqueous solution.

**Keywords:** adsorption, chloroanthraquinone, colorimetric sensor, copper ion, montmorillonite

## 1. Introduction

Copper is a heavy metal that is considered one of the most toxic contaminants in soil and water resources. The effects on human health caused by copper include liver damage, Wilson disease, Alzheimer's disease, etc. (Borchard *et al.*, 2018; Roberts, 2011; Squitti *et al.*, 2018). The maxi-mum permissible limit for copper in drinking water, set by the World Health Organization (WHO), is 2 mg/L (Datta, Uslu, & Kumar, 2015; Uddin, 2017). Therefore, it is necessary to clean metal-contaminated waste waters before discharge to the environment.

There are many techniques for the treatment of waste water contaminated by heavy metals, such as chemical precipitation, solvent extraction, membrane filtration, ion exchange, electrochemical removal and coagulation (Fan, Zhou, Jiang, Huang, & Lang, 2014; Rasouli, Aber, Salari, & Khataee, 2014). However, adsorption is considered an efficient, simple and low-cost technique (Shirzad-Siboni, Kha taee, Hassani, & Karaca, 2015; Wu *et al.*, 2011). Many studies have reported the adsorption of metallic ions from water by various adsorbents, such as activated carbon, zeolite and clay mineral (Burakov *et al.*, 2018; Uddin, 2017).

Clay minerals are hydrous aluminosilicates, sometimes with variable amounts of alkali metals, alkaline earth metals and other cations (Bhattacharyya & Gupta, 2008; Uddin, 2017). Typical characteristics of clay minerals are high specific surface area, high cation exchange capacity (CEC), chemical and mechanical stability, as well as low cost (Gonçalves dos Santos, Grassi, & Abate, 2015). During the past decades, studies of metal ion adsorption by clay minerals have mainly focused on montmorillonite (Mt). Abdellaoui *et al.* (2019) studied adsorption of divalent heavy metals by commercial montmorillonite and reported that the $Cu^{2+}$ adsorption

*Corresponding author
Email address: duangratth@nu.ac.th

capacity increases with pH of the solution. This behavior can be attributed to the surface charge of the clays and the competition between the $H^+$ and the divalent ions for the adsorption sites at a low pH. However, when the pH increases, the clay gets a negative surface charge, and the repulsive force decreases. Therefore the removal of $Cu^{2+}$ increases. The adsorption and separation of $Cu^{2+}$ from an aqueous solution using montmorillonite has been investigated by Datta *et al.* (2015). In the kinetic experiments, the maxi-mum adsorption capacity for the separation of $Cu^{2+}$ ions from aqueous solution was found (by employing the Langmuir model) to be 2.6260 mg/g. However, little has been reported on use of modified-Mt with colorimetric sensor to detect $Cu^{2+}$ in aqueous solution, and on its optimal adsorption capacity of $Cu^{2+}$.

The purposes of this present study are to compare the adsorption capacities of $Cu^{2+}$ ions in aqueous solution between Mt and Mt modified with alkylamine chloro-anthraquinone for a colorimetric sensor, or Mt-L, and to evaluate the adsorption parameters such as adsorbent dosage, pH and $Cu^{2+}$ ion concentration. In addition, the color, the adsorption kinetics and the adsorption isotherm were deter-mined to understand the adsorption mechanism of $Cu^{2+}$ ions on modified-Mt surfaces.

## 2. Materials and Methods

### 2.1 Materials

Montmorillonite-K10 (CEC 120 cmol/kg) and Cu $(NO_3)_2 \cdot 3H_2O$ were purchased from Sigma Aldrich. All of the solvents used were of analytical grade and they were purified by distillation under nitrogen gas before use. The colorimetric sensor L was synthesized according to the literature (Kaur & Kumar, 2008; Ranyuk *et al.*, 2011) by using the substitution reaction between 1,8-dichloroanthraquinone (0.40 g, 1.5 mmol) and 2-picolylamine (0.22 mL, 2 mmol) with $K_2CO_3$ (0.30 g, 2 mmol) in toluene (40 mL). The mixture solution was refluxed for 2-3 days under nitrogen atmosphere. Initially the solution was yellow and upon heating turned to red. Then, the solvent was removed under reduced pressure. The residue was dissolved in $CH_2Cl_2$, and 3M HCl was added to adjust pH to 1. The resulting residue was extracted with $CH_2Cl_2$ and water. The organic phase was dried over anhydrous $Na_2SO_4$, filtered and evaporated. The crude residue was purified by column chromatography ($SiO_2$, $CH_2Cl_2$) to yield a red solid (45%). The final product was characterized by FTIR, $^1$H-NMR and $^{13}$C-NMR spectroscopic techniques.

### 2.2 Characterization techniques

The functional groups of Mt and Mt-L were recorded by attenuated total reflection Fourier transform infrared spectroscopy (ATR-FTIR) on a PerkinElmer in the spectral range 4000-400 $cm^{-1}$. The X-ray diffraction patterns were recorded with a Panalytical XRD instrument over the 2θ value range 5-80 degrees, using Cu $K_\alpha$ radiation at $\lambda = 0.154$ nm. The absorbance of $Cu^{2+}$ was measured with a SPECORD 200 PLUS UV-Vis spectrophotometer over the wavelength range 200-1000 nm.

### 2.3 Modification of Mt

The synthesis of L modified Mt (Mt-L) was done in a 250 mL volumetric flask by dispersing 6 g of Mt in 1.5:1 ratio of $CH_3CN$:$H_2O$ for 2 h at room temperature, using a magnetic stirrer. Then, $6.00\times10^{-5}$ M of L in the same ratio of solvent was added to Mt dispersion. The mixture was then adjusted for pH with 0.1 M NaOH and 0.1 M HCl while stirring for 2 h. After that, the colloidal solution was centrifuged for 5 min at 4000 rpm and the precipitate was dried in an oven at 80°C to obtain the red-orange solid Mt-L.

### 2.4 Adsorption of $Cu^{2+}$ on the MT-L

All the adsorption experiments were prepared by adding 3.00 mL of $Cu^{2+}$ ion solution to Mt-L in seven PP bottles at room temperature. The colloidal solutions were stirred at 150 rpm for various times (0, 5, 15, 30, 45, 60, 90, 120 min). Each sample was centrifuged at 4000 rpm for 5 min to remove the Mt-L. The supernatant was measured in the range 200-1000 nm using a double beam UV-Vis spectro-photometer. The concentrations of $Cu^{2+}$ after adsorption were calculated with a calibration curve at $\lambda_{max}$ 800 nm. Each experiment was done three times.

To determine the effects of various parameters, adsorption experiments were run with varied adsorbent amounts from 4.00 to 40.0 g/L, at initial pH from 3 to 5, and initial $Cu^{2+}$ concentrations from $2.50\times10^{-3}$ to $4.50\times10^{-3}$ M. The $Cu^{2+}$ adsorption capacity by Mt-L was calculated from the amount of $Cu^{2+}$ adsorbed by the Mt-L ($q_t$ and $q_e$), and the percentage of removal efficiency was estimated, as shown in equations (1), (2) and (3).

$$q_t = \frac{(C_i - C_t)V}{M} \quad (1)$$

$$q_e = \frac{(C_i - C_e)V}{M} \quad (2)$$

$$\%\ \text{removal efficiency} = \frac{C_i - C_t}{C_i} \times 100 \quad (3)$$

Here $q_t$ and $q_e$ are the amounts of adsorbed metal per gram of clay at the observing time and at equilibrium (mg/g). $C_i$, $C_t$ and $C_e$ are the concentrations in solution initially, at the observing time, and at equilibrium (mg/L). V is the volume of metal ion solution (L) and M is the total amount of Mt-L (g) (Datta *et al.*, 2015).

The $Cu^{2+}$ concentration was varied from $2.50\times10^{-3}$ to $4.50\times10^{-3}$ M with Mt-L at 40.0 g/L and pH 5. To describe the adsorption kinetics, the pseudo-first and pseudo-second order models were fit by using linear and non-linear regression methods. The non-linear form of pseudo-first order kinetics is as follows:

$$q_t = q_e(1 - e^{-k_1 t}) \quad (4)$$

The pseudo-second order kinetic model assumes that chemical adsorption is the main rate-determining step and the overall rate of adsorption process seems to be controlled by the chemical process through exchange of electrons between adsorbent and adsorbate (Tiwari, Lalhmunsiama, Choi, & Lee, 2014). The non-linear form of pseudo-second order kinetics is as follows:

$$q_t = \frac{k_2 q_e^2 t}{1 + k_2 q_e t} \quad (5)$$

Here, $k_1$ (1/min) and $k_2$ (g/mg·min) are the pseudo-first order and pseudo-second order rate constant, respectively.

The adsorption isotherm was investigated by using linear and non-linear regression to fit data with Langmuir and Freundlich isotherm models. The Langmuir isotherm describes chemisorption and monolayer coverage of adsorbates onto adsorbents (Baseri & Tizro, 2017; Hu *et al.*, 2017a; Hu, Zhu, Cai, Hu, & Fu, 2017b). Its non-linear form is as follows:

$$q_e = \frac{q_m K_L C_e}{1 + K_L C_e} \quad (6)$$

The Freundlich isotherm assumes exponential distribution of active sites and their energies, including surface heterogeneity of the adsorbents. Its non-linear form is as follows:

$$q_e = K_F C_e^{1/n} \quad (7)$$

Here $q_m$ (mg/g) is the maximum monolayer adsorption capacity, $K_L$ and $K_F$ are the Langmuir and Freundlich constants, respectively, and n is the intensity of adsorption. Values of 1/n less than 1 represent favorable chemical adsorption conditions (Baseri & Tizro, 2017; Hu *et al.*, 2018; Tiwari *et al.*, 2014).

## 3. Results and Discussion

### 3.1 Modification of Mt

The structures of Mt and modified-Mt were confirmed by ATR-FTIR technique (Figure 1). A broad band around 3626 $cm^{-1}$ for Mt represents the hydroxyl group stretching vibrations of $Al_2OH$ group of the octahedral layer in Mt. The intense peak at 1027 $cm^{-1}$ was attributed to stretching vibrations of siloxane group in Si-O of Mt. After the modification, the peak for this functional group was shifted to the lower wavenumber 1013 $cm^{-1}$. These results prove the successful adsorption of L onto Mt surfaces (Shirzad-Siboni *et al.*, 2015). However, while there was a slight shift of wavenumbers, the retention of all parent montmorillonite bands clearly shows that the basic clay layer structure remains unaffected on adsorption (Molu & Yurdakoc, 2010). The XRD spectrum (Figure 2) showed the reflection of Mt at 8.88 degrees (1.99 nm) that corresponds to the basal spacing in 001 direction. In the case of Mt-L, this peak was slightly shifted to a lower angle at 8.83 degrees (2.00 nm). However, the adsorption could be observed by the color change of Mt-L solid from white to red-orange when L was intercalated between Mt layers.

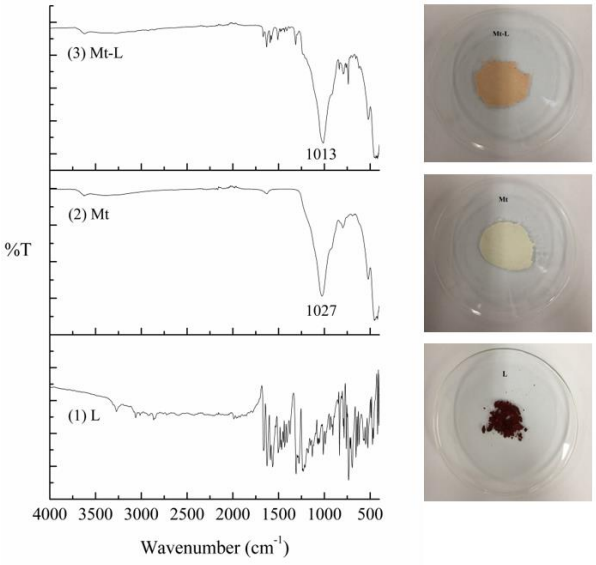


Figure 1. The ATR-FTIR spectra of (1) L (2) Mt and (3) Mt-L

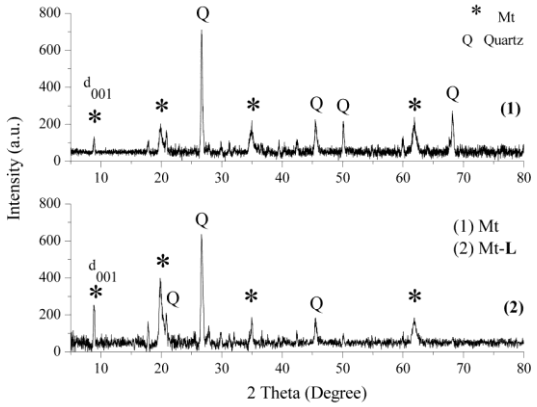


Figure 2. The XRD spectra of (1) Mt and (2) Mt-L

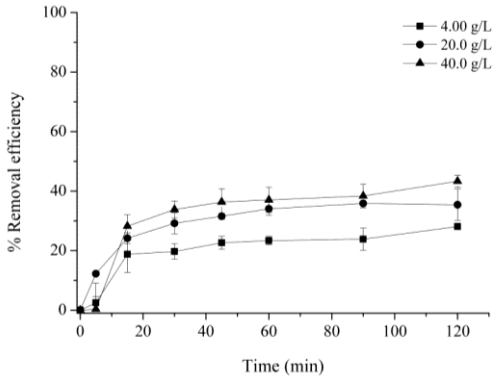


Figure 3. The effects of Mt-L amount on the removal of $Cu^{2+}$ ([$Cu^{2+}$] $3.50\times10^{-3}$ M)

### 3.2 The effects of Mt-L amount on $Cu^{2+}$ adsorption

The Mt-L in the range of 4.00 to 40.0 g/L was tested for the adsorption of $3.50\times10^{-3}$ M $Cu^{2+}$ measured at $\lambda_{max}$ 800 nm by UV-Vis spectroscopic technique, and the removal efficiency of $Cu^{2+}$ was calculated by using equation (3). The $Cu^{2+}$ removal efficiency (Figure 3) increased from 4.00 to 40.0 g/L of Mt-L because more sites are available for adsorption with increasing adsorbent amount. Moreover, the contact time from 0 to 15 min displayed the maximum adsorption rate. This may be due to the abundance of free surface of Mt-L to adsorb the $Cu^{2+}$ at the beginning**.** Then adsorption rate was constant after 15 min because of the repulsion forces between positive charge of adsorbate and the decrease in free active sites of Mt-L.

### 3.3 The effects of pH on $Cu^{2+}$ adsorption

The surface of clay is strongly affected by pH of the exchange solution and becomes negatively charged when pH increases (Abdellaoui *et al.*, 2019). In a previous study, an anthracene-9,10-dione based chromogenic sensor was designed, which possessed three amine nitrogens (alkyl amine, pyridyl amine and aryl amine) with distinctly different $pK_a$ values. The chemosensor showed pH dependent color changes with $Cu^{2+}$ at pH 4.0 (Kaur & Kumar, 2008). Therefore, the removal of $Cu^{2+}$ from aqueous solution not only depends on negative charges of Mt surface, but also largely depends on L properties. In an acidic solution, the N donor atoms of L were protonated and deprotonated after $Cu^{2+}$ was added. Moreover, the solution containing the soluble $Cu(NO_3)_2{\cdot}3H_2O$ is made basic with sodium hydroxide. Copper (II) hydroxide, $Cu(OH)_2$, of light-blue color, precipitates from the solution (Singh, Ojha, & Srivastava, 2009).

$$Cu(NO_3)_{2(aq)} + 2NaOH_{(aq)} \rightarrow Cu(OH)_{2(s)} + NaNO_{3(aq)}$$

Therefore, the effect of pH on the $Cu^{2+}$removal efficiency was investigated at acidic pH values ranging from 3 to 5 with $3.50\times10^{-3}$ M of $Cu^{2+}$ and 40.0 g/L of Mt-L (Figure 4). The results displayed the maximum removal efficiency at pH 5. Therefore, Mt-L could adsorb $Cu^{2+}$ well at mildly acidic conditions. However, pH less than 5 caused a decrease in the removal efficiency from 54% to 43% at 120 min, because the Mt-L surface became net positively charged so that there was electrostatic repulsion of the $Cu^{2+}$ (Tiwari *et al.*, 2014).

### 3.4 The effects of $Cu^{2+}$ concentration

The effects of $Cu^{2+}$ concentration on the removal efficiency were examined at initial $Cu^{2+}$ concentrations from $2.50\times10^{-3}$ to $4.50\times10^{-3}$ M using Mt-L of 40.0 g/L at an initial pH of 5.0 (Figure 5). An increase in the $Cu^{2+}$ concentration from $3.50\times10^{-3}$ to $4.50\times10^{-3}$ M decreased the removal of $Cu^{2+}$ from 54% to 40% at 120 min. The results are in agreement with previous reports indicating that at low concentrations of adsorbate, an excess of active sites was available for adsorption (Derakhshani & Naghizadeh, 2018; Tiwari *et al.*, 2014); so a decrease in the removal efficiency was obtained at higher $Cu^{2+}$ concentrations due to the limited number of active sites on Mt-L surfaces. However, the removal efficiency had no significant differences between $2.50\times10^{-3}$ and $3.50\times10^{-3}$ M.

### 3.5 Adsorption kinetics and adsorption isotherm studies

The adsorption kinetics were studied by using linear and non-linear forms of pseudo-first order and pseudo-second order models. The non-linear least-squares curve fitting used the Solver, Excel's powerful optimization package. The adsorption data of different $Cu^{2+}$concentrations were best fit with the pseudo-second order in linear form, with $R^2 = 0.9963$-0.9888, and exhibited higher $R^2$ than the non-linear form (Figure 6). Moreover, when the initial $Cu^{2+}$ concentration increased from $2.50\times10^{-3}$ to $3.50\times10^{-3}$ M, the values of $q_e$ increased, which corresponds to this model that describes the chemical adsorption through coordinated covalent bonds between Mt-L and $Cu^{2+}$, and electrostatic forces between negative charges of clay surfaces and positive charge of $Cu^{2+}$.

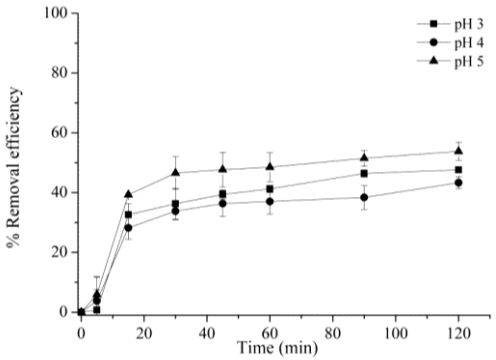


Figure 4. The effect of pH on the removal of $Cu^{2+}$ ($[Cu^{2+}]$ $3.50\times10^{-3}$ M and Mt-L 40.0 g/L)

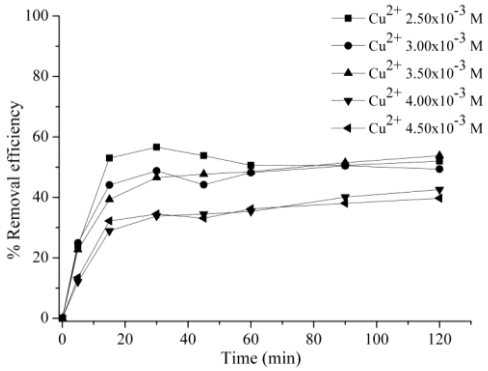


Figure 5. The effects of initial $Cu^{2+}$ concentration on the removal of $Cu^{2+}$ by Mt-L (Mt-L 40.0 g/L and pH 5)

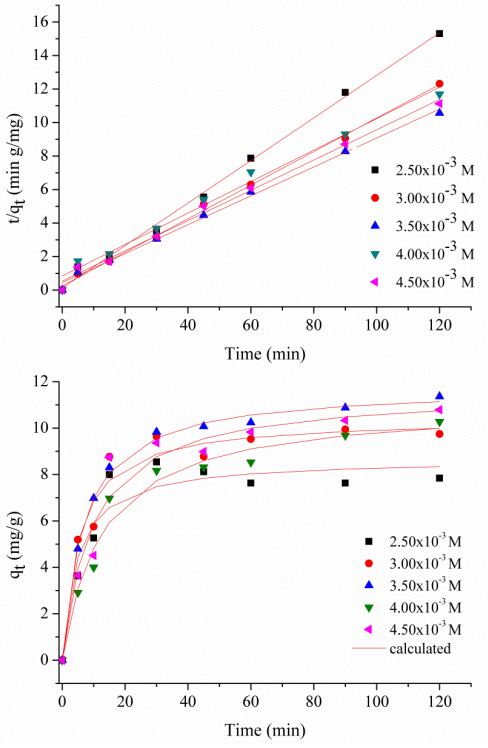


Figure 6. The linear and non-linear plots of pseudo-second order model for $Cu^{2+}$ removal by Mt-L (Mt-L 40.0 g/L and pH 5)

The kinetic parameters obtained from the linear and non-linear regression are summarized in Table 1.

The adsorption isotherms were evaluated using the models of Langmuir and Freundlich (Figure 7) and the adsorption parameters are presented in Table 2. The best model for the adsorption of $Cu^{2+}$ was Langmuir isotherm with $R^2$ = 0.9541 for the linear regression that describes the chemi-sorption and monolayer coverage of $Cu^{2+}$ onto Mt-L. In addition, the value of 1/n being less than 1 (0.0612) confirmed that the adsorption of $Cu^{2+}$ ions onto adsorbent surface was chemically favorable.

### 3.6 Comparative study of $Cu^{2+}$ removal by Mt and Mt-L

The comparison between Mt and Mt-L regarding $Cu^{2+}$ removal efficiency was performed with an initial $Cu^{2+}$ concentration of $3.50\times10^{-3}$ M, 40.0 g/L of adsorbent and an initial pH of 5.0. From the obtained data, the adsorption of $Cu^{2+}$ was high in the presence of L on Mt surfaces with 54% removal efficiency, while Mt gave 36% (Figure 8). The maximum adsorption capacity ($q_m$) determined from the Langmuir model was 9.5511 mg/g which was higher than that of $Cu^{2+}$ on Mt with $q_m$ estimate 7.5643 mg/g. This may be because L could coordinate with $Cu^{2+}$ via coordinated covalent bonds that improved the adsorption capacity. In agreement with previous reports, the adsorption of $Cu^{2+}$ on montmorillonite has been shown to follow Langmuir isotherm with $q_m$ at 7.6160 mg/g (Ijagbemi, Baek, & Kim, 2009), 2.6260 mg/g (Datta *et al.*, 2015) and the adsorption capacity was increased by surface modification (Sdiri, Higashi, Hatta, Jamoussi, & Tase, 2011; Wu *et al.*, 2011). Moreover, Mt-L gave a naked-eye detectable color change from red-orange to blue upon the adsorption of 10 mg/L $Cu^{2+}$ (Figure 9) because $Cu^{2+}$ can induce deprotonation of NH group of L, causing an internal charge transfer (ICT), which can be observed as the color change from red-orange to blue (Wu, Huang, & Du, 2009). These results confirmed the interaction between $Cu^{2+}$ and modified Mt surface while the binding between Mt and $Cu^{2+}$ without L did not show any color change.

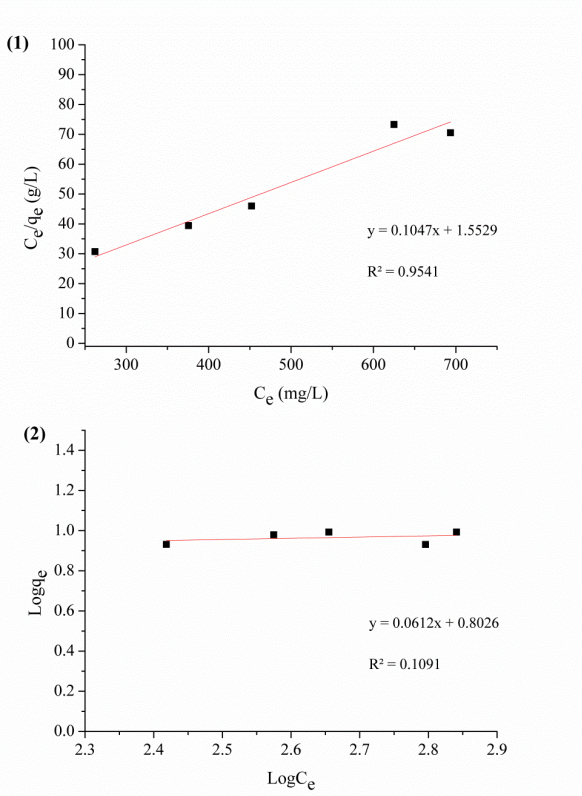


Figure 7. The linear plots of (1) Langmuir isotherm and (2) Freundlich isotherm for $Cu^{2+}$ adsorption by Mt-L ([$Cu^{2+}$] 2.50-4.50×$10^{-3}$ M, Mt-L 40.0 g/L, pH 5)

Table 1. The kinetic parameters obtained by linear and non-linear regression for both kinetic models

| $Cu^{2+}$ ×$10^{-3}$ (M) | $q_{e(exp)}$ (mg/g) | Linear regression | | | | | |
|---|---|---|---|---|---|---|---|
| | | pseudo-first order model | | | pseudo-second order model | | |
| | | $k_1$ (1/min) | $q_{e(cal)}$ (mg/g) | $R^2$ | $k_2$ (g/mg·min) | $q_{e(cal)}$ (mg/g) | $R^2$ |
| 2.50 | 8.5395 | -0.0150 | - | 0.3476 | 0.0713 | 7.9491 | 0.9955 |
| 3.00 | 8.7226 | -0.0129 | - | 0.3465 | 0.0279 | 10.1010 | 0.9962 |
| 3.50 | 9.8303 | -0.0145 | - | 0.4879 | 0.0156 | 11.6279 | 0.9963 |
| 4.00 | 8.1642 | -0.0145 | - | 0.4743 | 0.0086 | 10.8342 | 0.9838 |
| 4.50 | 9.3629 | -0.0143 | - | 0.2893 | 0.0113 | 11.2994 | 0.9888 |

| $Cu^{2+}$ ×$10^{-3}$ (M) | $q_{e(exp)}$ (mg/g) | Non-linear regression | | | | | | | |
|---|---|---|---|---|---|---|---|---|---|
| | | pseudo-first order model | | | | pseudo-second order model | | | |
| | | $k_1$ (1/min) | $q_{e(cal)}$ (mg/g) | $R^2$ | SSD | $k_2$ (g/mg·min) | $q_{e(cal)}$ (mg/g) | $R^2$ | SSD |
| 2.50 | 8.5395 | 0.1250 | 8.3064 | 0.9327 | 2.7155 | 0.0242 | 8.6674 | 0.8931 | 4.9923 |
| 3.00 | 8.7226 | 0.1194 | 8.7900 | 0.9990 | 2.6809 | 0.0184 | 10.4251 | 0.9579 | 3.2312 |
| 3.50 | 9.8303 | 0.1078 | 10.5857 | 1.0139 | 1.2786 | 0.0124 | 11.7734 | 0.9919 | 0.3186 |
| 4.00 | 8.1642 | 0.0681 | 9.4334 | 0.9777 | 3.1338 | 0.0070 | 11.0777 | 0.9579 | 2.4451 |
| 4.50 | 9.3629 | 0.0847 | 10.1523 | 0.9437 | 5.1436 | 0.0088 | 11.6185 | 0.9261 | 5.5744 |

Table 2. The fitted parameters for Langmuir and Freundlich isotherms for the removal of $Cu^{2+}$

| | Langmuir isotherm | | | | Freundlich isotherm | | | |
|---|---|---|---|---|---|---|---|---|
| | $q_m$ (mg/g) | $K_L$ (L/mg) | $R^2$ | SSD | $K_F$ (mg·L/g) | n | $R^2$ | SSD |
| Linear | 9.5511 | 0.0674 | 0.9541 | - | 6.3475 | 16.3399 | 0.1091 | - |
| Non-linear | 9.9172 | 0.0320 | 0.1443 | 1.5079 | 6.4046 | 16.6448 | 0.1068 | 1.5853 |

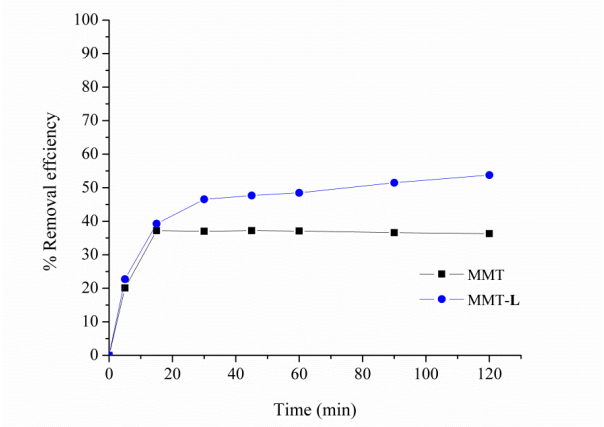


Figure 8. The comparison of $Cu^{2+}$ removal efficiency between Mt and Mt-L. ([$Cu^{2+}$] $7.00\times10^{-3}$ M, Mt-L 40.0 g/L and pH 5)

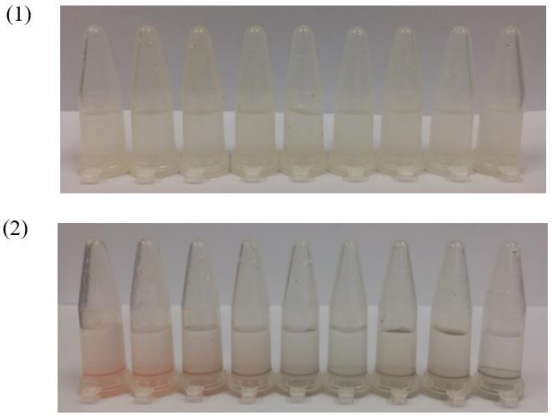


Figure 9. Color of (1) Mt and (2) Mt-L (3.00 g/L) in the presence of 1 mL $Cu^{2+}$ solution (from left to right: $Cu^{2+}$ 0, 1, 5, 10, 20, 30, 40, 50 and 500 mg/L)

## 4. Conclusions

Montmorillonite was modified with alkylamine chloroanthraquinone for use as adsorbent and colorimetric sensor to separate and detect $Cu^{2+}$ in an aqueous solution. The results showed the maximum adsorption efficiency of 54% with an initial $Cu^{2+}$ concentration of $3.50\times10^{-3}$ M, 40.0 g/L of Mt-L and an initial pH of 5.0. The adsorption results could be confirmed by naked-eye as well, due to a color change from red-orange to blue upon addition of $Cu^{2+}$ to colloidal solution of Mt-L. The adsorption kinetics fit by linear regression of the pseudo-second order model gave $R^2 = 0.99$, indicating chemical adsorption. The adsorption equilibrium was well fit by the Langmuir isotherm based on the assumption of monolayer coverage on homogeneous adsorbent. The maximum adsorption capacity ($q_m$) was estimated to be 9.5511 mg/g, which is higher than in some previous reports. Therefore, Mt-L has great potential as an adsorbent and a powerful colorimetric sensor for $Cu^{2+}$ ions in an aqueous solution.

## Acknowledgements

Financial support for Undergraduate Thesis has been provided by the Department of Chemistry, Faculty of Science, Naresuan University.

## References

Abdellaoui, Y., Olguín, M. T., Abatal, M., Ali, B., Díaz Méndez, S. E., & Santiago, A. A. (2019). Comparison of the divalent heavy metals (Pb, Cu and Cd) adsorption behavior by montmorillonite-KSF and their calcium- and sodium-forms. *Superlattices and Microstructures*, *127*, 165-175. doi:10.1016/j.spmi.2017.11.061

Baseri, H., & Tizro, S. (2017). Treatment of nickel ions from contaminated water by magnetite based nano composite adsorbents: Effects of thermodynamic and kinetic parameters and modeling with Langmuir and Freundlich isotherms. *Process Safety and Environmental Protection*, *109*, 465-477. doi:10.1016/j.psep.2017.04.022

Bhattacharyya, K. G., & Gupta, S. S. (2008). Adsorption of a few heavy metals on natural and modified kaolinite and montmorillonite: A review. *Advances in Colloid and Interface Science*, *140*, 114-131. doi:10.1016/j.cis.2007.12.008

Borchard, S., Bork, F., Rieder, T., Eberhagen, C., Popper, B., Lichtmannegger, J., . . . Zischka, H. (2018). The exceptional sensitivity of brain mitochondria to copper. *Toxicology in Vitro*, *51*, 11-22. doi:10.1016/j.tiv.2018.04.012

Burakov, A. E., Galunin, E. V., Burakova, I. V., Kucherova, A. E., Agarwal, S., Tkachev, A. G., & Gupta, V. K. (2018). Adsorption of heavy metals on conventional and nanostructured materials for wastewater treatment purposes: A review. *Ecotoxicology and Environmental Safety*, *148*, 702-712. doi:10.1016/j.ecoenv.2017.11.034

Datta, D., Uslu, H., & Kumar, S. (2015). Adsorptive separation of $Cu^{2+}$ from an aqueous solution using trioctylamine supported montmorillonite. *Journal of Chemical and Engineering Data*, *60*, 3193-3200. doi:10.1021/acs.jced.5b00413

Derakhshani, E., & Naghizadeh, A. (2018). Optimization of humic acid removal by adsorption onto bentonite and

montmorillonite nanoparticles. *Journal of Molecular Liquids*, *259*, 76-81. doi:10.1016/j.molliq.2018.03.014

Fan, H., Zhou, L., Jiang, X., Huang, Q., & Lang, W. (2014). Adsorption of $Cu^{2+}$ and methylene blue on dodecyl sulfobetaine surfactant-modified montmorillonite. *Applied Clay Science*, *95*, 150-158. doi:10.1016/j.clay.2014.04.001

Gonçalves dos Santos, V. C., Grassi, M. T., & Abate, G. (2015). Sorption of Hg(II) by modified K10 montmorillonite: Influence of pH, ionic strength and the treatment with different cations. *Geoderma*, *237-238*, 129-136. doi:10.1016/j.geoderma.2014.08.018

Hu, C., Li, G., Wang, Y., Li, F., Guo, G., & Hu, H. (2017a). The effect of pH on the bonding of $Cu^{2+}$and chitosan-montmorillonitecomposite. *International Journal of Biological Macromolecules*, *103*, 751-757. doi:10.1016/j.ijbiomac.2017.05.065

Hu, C., Zhu, P., Cai, M., Hu, H., & Fu, Q. (2017b). Comparative adsorption of Pb(II), Cu(II) and Cd(II) on chitosan saturated montmorillonite: Kinetic, thermodynamic and equilibrium studies. *Applied Clay Science*, *143*, 320-326. doi:10.1016/j.clay.2017.04.005

Hu, W., Lu, S., Song, W., Chen, T., Hayat, T., Alsaedi, A. S., . . . Liu, H. (2018). Competitive adsorption of U(VI) and Co(II) on montmorillonite: A batch and spectroscopic approach. *Applied Clay Science*, *157*, 121-129. doi:10.1016/j.clay.2018.02.030

Ijagbemi, C. O., Baek, M. H., & Kim, D. S. (2009). Montmorillonite surface properties and sorption characteristics for heavy metal removal from aqueous solutions, *Journal of Hazardous Materials*, *166*, 538-546. doi:10.1016/j.jhazmat.2008.11.085

Kaur, N., & Kumar, S. (2008). A differential receptor for selective and quantitative multi-ion analysis for $Co^{2+}$ and $Ni^{2+}/Cu^{2+}$. *Tetrahedron Letters*, *49*, 5067-5069. doi:10.1016/j.tetlet.2008.06.023

Molu, Z. B., & Yurdakoc, K. (2010). Preparation and characterization of aluminum pillared K10 and KSF for adsorption of trimethoprim. *Microporous and Mesoporous Materials*, *127*, 50-60. doi:10.1016/j.micromeso.2009.06.027

Ranyuk, E., Uglov, A., Meyer, M., Lemeune, A.B., Denat, F., Averin, A., . . . Guilard, R. (2011). Rational design of aminoanthraquinones for colorimetric detection of heavy metal ions in aqueous solution. *Dalton Transactions*, *40*, 10491-10502. doi:10.1039/c1dt10677e

Rasouli, F., Aber, S., Salari, D., & Khataee, A. R. (2014). Optimized removal of Reactive Navy Blue SP-BR by organo-montmorillonite based adsorbents through central composite design. *Applied Clay Science*, *87*, 228-234. doi:10.1016/j.clay.2013.11.010

Roberts, E. A. (2011). Wilson's disease. *Medicine*, *39*, 602-604. doi:10.1016/j.mpmed.2011.08.006

Sdiri, A., Higashi, T., Hatta, T., Jamoussi, F., & Tase, N. (2011). Evaluating the adsorptive capacity of montmorillonitic and calcareous clays on the removal of several heavy metals in aqueous systems. *Chemical Engineering Journal*, *172*, 37-46. doi:10.1016/j.cej.2011.05.015

Shirzad-Siboni, M., Khataee, A., Hassani, A., & Karaca, S. (2015). Preparation, characterization and application of a CTAB-modified nanoclay for the adsorption of an herbicide from aqueous solutions: Kinetic and equilibrium studies. *Comptes Rendus Chimie*, *18*, 204-214. doi:10.1016/j.crci.2014.06.004

Singh, D. P., Ojha, A. K. & Srivastava, O. N. (2009). Synthesis of different $Cu(OH)_2$ and CuO (nanowires, rectangles, seed-, belt-, and sheetlike) nanostructures by simple wet chemical route. *The Journal of Physical Chemistry C*, *113*, 3409-3418. doi:10.1021/jp804832g

Squitti, R., Ghidoni, R., Simonelli, I., Ivanova, I. D., Colabufo, N. A., Zuin, M., . . . Siotto, M. (2018). Copper dyshomeostasis in Wilson disease and Alzheimer's disease as shown by serum and urine copper indicators. *Journal of Trace Elements in Medicine and Biology*, *45*,181-188. doi:10.1016/j.jtemb.2017.11.005

Tiwari, D., Lalhmunsiama, Choi, S. I., & Lee, S. M. (2014). Activated sericite: An efficient and effective natural clay material for attenuation of cesium from aquatic environment. *Pedosphere*, *24*(6), 731-742. doi:10.1016/S1002-0160(14)60060-6

Uddin, M. K. (2017). A review on the adsorption of heavy metals by clay minerals, with special focus on the past decade. *Chemical Engineering Journal*, *308*, 438-462. doi:10.1016/j.cej.2016.09.029

Wu, P., Zhang, Q., Dai, Y., Zhu, N., Dang, Z., Li, P., . . . Wang, X. (2011). Adsorption of Cu(II), Cd(II) and Cr(III) ions from aqueous solutions on humic acid modified Ca-montmorillonite. *Geoderma*, *164*, 215-219. doi:10.1016/j.geoderma.2011.06.012

Wu, S. P., Huang, R. Y., & Du, K. J. (2009). Colorimetric sensing of Cu(II) by 2-methyl-3-[(pyridin-2-ylmethyl)-amino]-1,4-naphthoquinone: Cu(II) induced deprotonation of NH responsible for color changes. *Dalton Transactions*, 4736-4740. doi: 10.1039/b822613j